Tensor Processing for Texture and Colour Segmentation

Rodrigo de Luis-García[1], Rachid Deriche[2], Mikael Rousson[2], and Carlos Alberola-López[1]

[1] ETSI Telecomunicación, University of Valladolid, Valladolid, Spain
{rodlui, caralb}@tel.uva.es
[2] Projet Odyssée, INRIA Sophia-Antipolis, France
{Rachid.Deriche, Mikael.Rousson}@sophia.inria.fr

Abstract. In this paper, we propose an original approach for texture and colour segmentation based on the tensor processing of the nonlinear structure tensor. While the tensor structure is a well established tool for image segmentation, its advantages were only partly used because of the vector processing of that information. In this work, we use more appropriate definitions of tensor distance grounded in concepts from information theory and compare their performance on a large number of images. We clearly show that the traditional Frobenius norm-based tensor distance is not the most appropriate one. Symmetrized KL divergence and Riemannian distance intrinsic to the manifold of the symmetric positive definite matrices are tested and compared. Adding to that, the extended structure tensor and the compact structure tensor are two new concepts that we present to incorporate gray or colour information without losing the tensor properties. The performance and the superiority of the Riemannian based approach over some recent studies are demonstrated on a large number of gray-level and colour data sets as well as real images.

1 Introduction

The segmentation of textured images usually relies on the extraction of suitable features from the image. Traditionally, Gabor filters have been used [3, 19], but they yield a lot of feature channels. This drawback was overcome by the use of the structure tensor [12, 1, 2] or its improved versions such as the *nonlinear structure tensor* (NLST) [6, 4].

After the features have been extracted, a segmentation method that employs this information has to be designed. Lately, level set-based methods [23, 18, 9, 10] have gained much relevance due to their good properties. Besides, they can easily integrate boundary, region and even shape prior information [18, 7, 20, 16, 8].

A very interesting method for the segmentation of textured images was proposed in [21], based on the features extracted by the NLST. The geodesic active regions model is applied to a vector-valued image whose channels are the components of the NLST, obtaining promising results. However, the advantages of the

H. Kalviainen et al. (Eds.): SCIA 2005, LNCS 3540, pp. 1117–1127, 2005.

structure tensor are partially lost because of the vector processing of that information. To our knowledge, no tensor processing has been applied to the structure tensor for texture segmentation. Nevertheless, much work has been done in the field of Diffusion Tensor Imaging (DTI) for the segmentation of tensor-valued images [24, 25, 14, 15, 22, 11]. Level-set based methods were used in [14, 15] for the segmentation of anatomical structures, employing intrinsic tensor dissimilarity measures based on geometric properties of their respective spaces.

In this paper, we propose a novel texture segmentation method which, based on the use of the NLST and its new extended versions for feature extraction, afterwards performs the segmentation in the tensor domain by applying region, level-set based tensor field segmentation tools developed for the segmentation of DTI [14, 15, 22, 25]. This way, the nice properties of the NLST for texture discrimination are fully exploited, as experimental results showed.

Furthermore, new modalities of structure tensor are also proposed that incorporate gray level or colour information while keeping the tensor structure. Altogether, comparative results are shown which indicate that the novel segmentation methods described in this paper yield excellent results and improve the state of the art.

The paper is organized as follows: next section studies the NLST for texture extraction. Afterwards, we review the vector adaptive segmentation methods employed in [21] for texture segmentation, and the tensor schemes proposed in [14, 15, 22] for DTI segmentation. In Section 4, we present the main contribution of this paper, that is, the tensor processing of the NLST for texture segmentation. Besides, we introduce new, improved modalities of the structure tensor incorporating gray or colour information. Section 5 describes the extensive experiments made to test and validate the methods proposed, followed by a discussion of the results. Finally, a brief summary is presented.

2 Nonlinear Structure Tensor

For a scalar image I, the structure tensor is defined as follows [12, 1, 2]:

$$J_\rho = K_\rho * (\nabla I \nabla I^T) = \begin{pmatrix} K_\rho * I_x^2 & K_\rho * I_x I_y \\ K_\rho * I_x I_y & K_\rho * I_y^2 \end{pmatrix} \tag{1}$$

where K_ρ is a Gaussian kernel with standard deviation ρ, and subscripts denote partial derivatives. For vector-valued images, the following expression is used :

$$J_\rho = K_\rho * \left(\sum_{i=1}^{N} \nabla I_i \nabla I_i^T \right) \tag{2}$$

The smoothing with a Gaussian kernel makes the structure tensor suffer from the dislocation of edges. To solve this problem, Brox and Weickert [4, 6] propose to replace the Gaussian smoothing by nonlinear diffusion. For vector-valued data, the diffusion equation becomes:

$$\partial_t u_i = \operatorname{div}\left(g\left(\sum_{k=1}^{N}|\nabla u_k|^2\right)\nabla u_i\right) \quad \forall i \tag{3}$$

where u_i is an evolving vector channel, and N is the total number of vector channels.

The NLST can be obtained, for a scalar image, by applying Eq. 3 with initial conditions $\mathbf{u} = [\, I_x^2 \quad I_y^2 \quad I_x I_y \,]^T$. In practice, however, the original image is added as an extra channel because it can provide valuable information, yielding $\mathbf{u} = [\, I_x^2 \quad I_y^2 \quad I_x I_y \quad I \,]^T$.However, it can be noticed that these components have not the same order of magnitude, which could cause some problems. To solve this problem and force all channels to take values in the same range, a simple normalization is not a good choice, since it would amplify the noise in channels containing no information. Instead, a better solution is to replace the structure tensor by its square root (see [17] for details).

3 Adaptive Segmentation

3.1 Vector Field Segmentation

In [21], a variational approach was proposed for the segmentation of textured images. Following the work in [19], the image segmentation can be found by maximizing the *a posteriori* partition probability $p(P(\Omega)|I)$ given the observed image I, where $P(\Omega) = \{\Omega_1, \Omega_2\}$ is the partition of the image domain Ω in two regions. This is equivalent to the minimization of an energy term. Two hypotheses are necessary: all partitions are equally probable, and the pixels within each region are independent. Then, if a Gaussian approximation is used to model each region, let $\{\mu_1, \Sigma_1\}$ and $\{\mu_2, \Sigma_2\}$ be the vectors means and the covariance matrices of the Gaussian approximation for Ω_1 and Ω_2. The partition boundary $\partial\Omega$ can be represented by the level set function Φ, and the resulting energy can then be minimized by iteratively estimating the optimal statistical parameters $\{\mu_i, \Sigma_i\}$ for a fixed level set function Φ and evolving the level set function with these parameters. The following system of coupled equations is obtained (see [21] for details):

$$\begin{cases} \mu_i = \frac{1}{|\Omega_i|}\int_{\Omega_i} u(x)dx, \\ \Sigma_i = \frac{1}{|\Omega_i|}\int_{\Omega_i}(u(x)-\mu_i)(u(x)-\mu_i)^T dx \\ \frac{\partial\Phi}{\partial t}(x) = \delta(\Phi)(\nu\operatorname{div}(\frac{\nabla\Phi}{|\nabla\Phi|}) + \log\frac{p_1(u(x))}{p_2(u(x))}) \end{cases} \tag{4}$$

where $\delta(z)$ is the Dirac function.

Considering identity covariance matrix leads to the well known piece-wise constant Chan-Vese model [7] while considering other covariance matrices (diagonal, full..) allows to discriminate between regions having the same mean but different second order statistics. Finally, if Gaussian approximation for some channels is not appropriate, an estimation of the probability density function based on the parzen window can be performed. [21].

3.2 Tensor Field Segmentation

The adaptive segmentation method shown above was designed for vector-valued images, and so the structure tensor has to be converted into a vector leading to the traditional Frobenius norm-based tensor distance. This way, the nice properties of the structure tensor as such are lost. Therefore, a tensor processing of the NLST would be expected to outperform the approach proposed in [21].

For the segmentation of Diffusion Tensor images, a symmetric positive definite (SPD) tensor was interpreted as a covariance matrix of a Gaussian distribution in Wang *et al.* [24, 25]. Then, the natural distance between two Gaussian pdfs, given by the symmetrized Kullback-Leibler distance, can be a measure of dissimilarity between two Gaussian distributions, represented by SPD tensors.

The symmetrized Kullback-Leibler distance (also called J-divergence) between two distributions p and q is given by:

$$d(p,q) = \frac{1}{2}\int (p(x)\log\frac{p(x)}{q(x)} + q(x)\log\frac{q(x)}{p(x)})dx \tag{5}$$

It is possible to obtain a very simple closed form for the symmetrized Kullback-Leibler distance [24]. Now, let us denote by $\mathbf{T_1}$ and $\mathbf{T_2}$ the mean values of the tensor image over the regions Ω_1 and Ω_2. It is possible to model the distribution of the KL distances to $\mathbf{T_1}$ and $\mathbf{T_2}$ in their respective domains by the densities $p_{d,1}$ and $p_{d,2}$. Making the assumption that $p_{d,1}$ and $p_{d,2}$ are Gaussian of zero mean and variances σ_1^2 and σ_2^2, the minimization of the corresponding energy functional can be achieved as follows [14, 15, 22]:

$$\begin{cases} \sigma_i = \frac{1}{|\Omega_i|}\int_{\Omega_i} p_{d,i}^2(x)dx \\ \frac{\partial \Phi}{\partial t}(x) = \delta(\Phi)(\nu div(\frac{\nabla \Phi}{|\nabla \Phi|}) + \frac{1}{2}\log\frac{p_{d,2}}{p_{d,1}}) \end{cases} \tag{6}$$

This approach has been successfully employed for Diffusion MRI segmentation in [15]. However, as shown in [14, 13], it only considers the parameterized *pdfs* as living in the linear space $\mathbb{R}^6$ instead of taking into account the Riemannian structure of the underlying manifold, thus being able to define a geodesic distance. It is not possible to find a closed form of the geodesic distance for general distributions, but a closed-form of the geodesic distance between two symmetric positive definite matrices can be found. Indeed, the Riemannian distance, intrinsic to the manifold of the symmetric positive definite matrices, between two SPD matrices P_1 and P_2 is shown to be equal to $d(P_1,P_2) = \sqrt{\sum_{i=1}^{n} ln^2(\lambda_1)}$ where $\lambda_i, i = 1..n$ are the positive eigenvalues of $P_1^{-1}P_2$.

Such an approach and its advantages were presented in [13] where the authors present impressive results on Diffusion Tensor MRI. In this work, we propose to replace the symmetrized KL distance with this Riemannian distance and compare their performance on segmenting textured, coloured images.

4 Tensor Processing for Segmentation

The NLST described in Section 2 has shown to be a very suitable way to extract texture information from images. It was employed for texture segmentation in [21] obtaining promising results, but the tensor structure of the texture representation was not exploited. To overcome this limitation, we propose a novel segmentation method for textured images, which, starting from the NLST, applies a tensor adaptive segmentation approach in order to take advantage of the nice properties of the structure tensor as such.

Let us consider an image I, containing at each pixel, instead of the scalar or vector value, the 2×2 nonlinear structure tensor described in Section 2:

$$\mathbf{T} = \begin{pmatrix} \hat{I_x^2} & \hat{I_x I_y} \\ \hat{I_x I_y} & \hat{I_y^2} \end{pmatrix} \tag{7}$$

$$\mathbf{T_C} = \sum_i \begin{pmatrix} \hat{(I_i)_x^2} & \hat{(I_i)_x (I_i)_y} \\ \hat{(I_i)_x (I_i)_y} & \hat{(I_i)_y^2} \end{pmatrix} \tag{8}$$

for gray level or colour images, respectively, where by $\hat{\cdot}$ we denote the nonlinearly diffused components.

For this tensor-valued image, we employ the adaptive segmentation methods based on the Kullback-Leibler and the geodesic distances proposed for the segmentation of DTI images [13, 14, 15] (see Section 3.2).

4.1 Advanced Tensor Architectures

The NLST is a very valuable feature for the segmentation of texture images, as will be shown in Section 5. However, when compared with the feature vector $\mathbf{u} = \begin{bmatrix} \hat{I_x^2} & \hat{I_y^2} & \hat{I_x I_y} & \hat{I} \end{bmatrix}^T$ employed in [21], it is clear that the tensor approach proposed in this paper has the disadvantage of not using any gray information (or colour information, in the case of vector-valued images) at all. Thus, it would be desirable to incorporate this valuable information without losing the nice properties of the NLST. To do so, we propose to use the *nonlinear extended structure tensor*, which, for a scalar image, we define as follows:

$$\mathbf{T_E} = vv^T = \begin{pmatrix} \hat{I_x^2} & \hat{I_x I_y} & \hat{I_x I} \\ \hat{I_x I_y} & \hat{I_y^2} & \hat{I_y I} \\ \hat{I_x I} & \hat{I_y I} & \hat{I^2} \end{pmatrix} \tag{9}$$

where $v = \begin{bmatrix} I_x & I_y & I \end{bmatrix}^T$.

With regard to colour images, the extended structure tensor is adapted and becomes $\mathbf{T_E} = ww^T$, where $w = \begin{bmatrix} I'_x & I'_y & I_R & I_G & I_B \end{bmatrix}^T$ and $I' = \frac{I_R + I_G + I_B}{3}$.

The *extended structure tensor* contains a lot of valuable information for the discrimination between different textures. However, the 3×3 tensor (5×5 for colour images) implies that the energy minimization has to be done in a higher

dimensional space, which can be too difficult and result in multiple local minima. To overcome this disadvantage, it would be desirable to reduce the tensor size without losing valuable information. This can be done using *Principal Component Analysis* (PCA). Using this transformation, it is possible to obtain $v' = \mathrm{PCA}(v) = [\, v'_1 \quad v'_2 \,]^T$, which will be afterwards used to construct the *nonlinear compact structure tensor* (see [17] for details):

$$\mathbf{T_C} = v'(v')^T = \begin{pmatrix} (\hat{v'_1})^2 & \hat{v'_1 v'_2} \\ \hat{v'_1 v'_2} & (\hat{v'_2})^2 \end{pmatrix} \tag{10}$$

For colour images, the same procedure can be used to reduce the 5×5 extended structure tensor to the 2×2 *compact structure tensor*.

In some cases, however, valuable information can be lost as the dimension reduction is very marked for the colour case (5×5 to 2×2). This can be solved by applying a dimensionality reduction to a size that keeps all the eigenvectors responsible for a minimum percentage of the total variance. Using this procedure a structure tensor of variable size is obtained, which is called *adaptive compact structure tensor*.

5 Experimental Results

We first tested the performance of the proposed methods with two synthetic test sets for gray-level and colour images, respectively. Starting from the Brodatz and the CUReT (Columbia Utrecht Reflectance and Texture Database) databases, 100 test images were created for each test set by combining two textures per image.

Different combinations of texture representation schemes and adaptive segmentation methods were tested. First, the vector processing of the NLST [21] was tested and considered as a performance reference, with two slightly different segmentation techniques (see Section 3.1). Next, the gray or colour channels were removed using the earlier vector approach. Afterwards, the tensor segmentation approaches proposed in this work were tested (KL distance and geodesic distance to the Riemannian barycenter, see Section 3.2), combined with the different structure tensors proposed (classical structure tensor, extended structure tensor, compact structure tensor and adaptive compact structure tensor).

The performance of the segmentation was measured in terms of a *success score*, defined as the relation between the number of pixels correctly classified and the total number of pixels. Obviously, $0 \leq S \leq 1$. In Table 1, we show the median values for all segmentation methods on the gray-value test set. Results for the colour test set are shown in Table 2.

As for the initial contour, small circular contours were placed all over the image. In Figure 1, the evolution of a segmentation process can be seen at different stages. The proposed methods were also tested using real-world images, showing excellent results for gray-level and colour images. Figure 2 shows some results on test images from [21, 5], which prove our method to be fully competitive.

Table 1. Results for the different segmentation methods for gray-level images

Texture representation	Segmentation method	Median Value
Feature vector 1×4	Gaussian full covariance	0.6624
	Gaussian uncorrelated	0.7079
	Gaussian-Parzen	0.7103
Feature vector 1×3 (no gray information)	Gaussian full covariance	0.6489
	Gaussian uncorrelated	0.5357
Structure tensor 2×2 (no gray information)	KL distance	0.7040
	Geodesic distance	0.7167
Extended tensor 3×3	KL distance	0.7405
	Geodesic distance	0.7925
Compact tensor 2×2	KL distance	0.7800
	Geodesic distance	0.8059

Table 2. Results for the different segmentation methods for colour images

Texture representation	Segmentation method	Median Value
Feature vector 1×6	Gaussian full covariance	0.7002
	Gaussian uncorrelated	0.8609
Feature vector 1×3 (no colour information)	Gaussian full covariance	0.6692
	Gaussian uncorrelated	0.7211
Structure tensor 2×2 (no colour information)	KL distance	0.8162
	Geodesic distance	0.8093
Extended tensor 5×5	KL distance	0.8459
	Geodesic distance	0.8549
Compact tensor 2×2	KL distance	0.8807
	Geodesic distance	0.8976
Adaptive Compact tensor 5% of variance	KL distance	0.9023
	Geodesic distance	0.9148

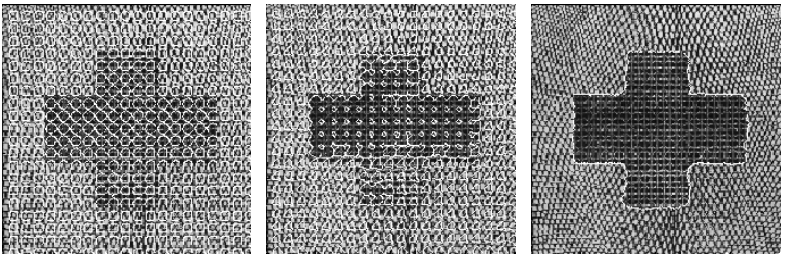

Fig. 1. Different samples of the segmentation process for a gray level image belonging to the test set, using the compact and adaptive compact structure tensor (5% of variance), respectively, and KL distance

The results, both for gray-level and colour images, show clearly that the tensor processing of the structure tensor can help improve the accuracy of the segmen-

Fig. 2. Segmentation results with gray-level and colour real-world images, using the compact structure tensor and KL distance

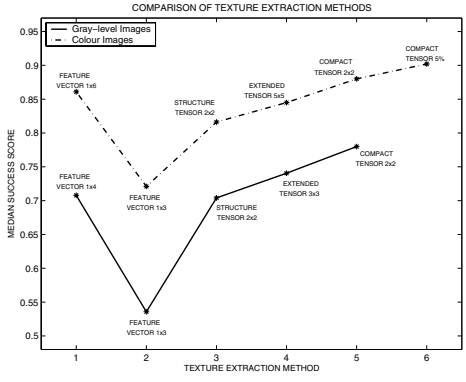

Fig. 3. Graphical comparison of the different texture representation schemes tested, for gray and colour images

tation over the vector processing of that structure tensor. This can be seen in Tables 1 and 2, and even more clearly in Figure 3. Indeed, all the relative performances clearly suggest that the tensor processing is more powerful than the vector counterpart. As with regard to the suitability of the proposed advanced tensor modalities, it can be seen in Figure 3 that, for a fixed tensor segmentation method, the use of the extended structure tensor slightly improves the performance over the classical structure tensor, for gray images. A bigger improvement is obtained for colour images. In both cases, there is a noticeable performance improvement if the compact tensor is used, as it keeps the space dimension low while retaining all the valuable information. For colour images, with the use of the adaptive compact tensor the best results in all can be reached.

Another interesting issue is the choice between the two tensor segmentation methods proposed, which is not so clear. In Figure 4 we show comparisons of the results for both methods, working on the different structure tensor architectures. In general, results favour the use of the geodesic distance to the Riemannian barycenter with respect to the use of the Kullback-Leibler distance. Anyway, the use of the geodesic distance is quite more computationally expensive that the KL option, mainly because the riemannian barycenter has to be computed using an iterative method. This drawback becomes a serious problem for extended tensor architectures, for which the KL distance should be preferred in most cases.

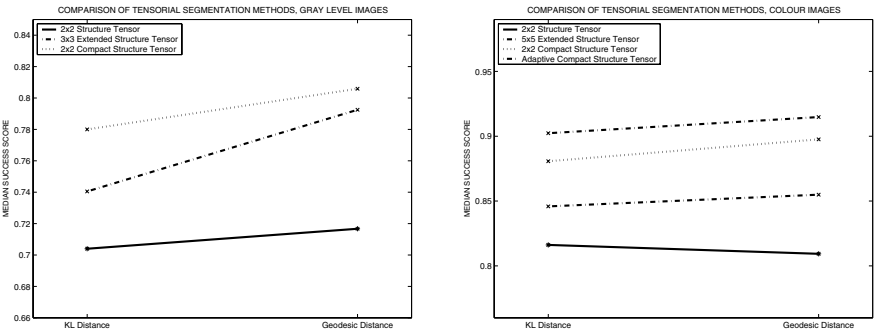

(a) (b)

Fig. 4. Graphical comparison of the different tensor adaptive segmentation methods tested, for gray (a) and colour images (b)

6 Summary

We have presented a NLST based approach for segmenting textured and coloured images. Various tensor field segmentation techniques, recently proposed for DT-MRI, have been employed and tested, showing that the tensor processing of the NLST significantly improves the segmentation performance with respect to more classical approaches based on the vector processing of such tensors. Moreover, it has been shown that the gray or colour information can be incorporated using the extended structure tensor, definitely boosting the segmentation accuracy. One step further was taken with the introduction of the compact structure tensor, which aims at reducing the size of the structure tensor while keeping all the valuable information. An adaptive compact tensor of variable size reaches the maximum refinement and yields results that improve the state of the art.

Acknowledgments

Our research is partly funded by the Imavis project numbered HPMT-CT-2000-00040 working within the framework of the *Marie Curie Fellowship Training Sites Programme*, as well as CICYT TIC 3808-C02-02, FP6-507609. This is gratefully acknowledged.

References

1. J. Bigun, G. H. Grandlund, and J. Wiklund, "Multidimensional orientation estimation with applications to texture analysis and optical flow," *IEEE Trans. on PAMI*, 13(8): 775-790, 1991.
2. J. Bigun, G. H. Grandlund "Optimal orientation detection of linear symmetry," *Proc. 1st IEEE ICCV, London, June 1987*
3. A. C. Bovik, M. Clark, and W. S. Geisler, "Multichannel texture analysis using localized spatial filters," *IEEE Trans. on PAMI*, 12(1): 55-73, 1990.

4. T. Brox and J. Weickert, "Nonlinear matrix diffusion for optic flow estimation," in *Proc. of the 24th DAGM Symp. , vol. 2449 of LNCS*, Zurich, Switzerland, sep 2002, pp. 446–453.
5. T. Brox, M. Rousson, R. Deriche, and J. Weickert, "Unsupervised segmentation incorporating colour, texture, and motion," INRIA, Research Rep. 4760, mar 2003.
6. T. Brox, J. Weickert, B. Burgeth, P. Mrázek "Nonlinear structure tensors", Preprint No. 113, Department of Mathematics, Saarland University, Saarbrücken, Germany. Oct. 2004
7. T. F. Chan and L. A. Vese, "Active contours without edges," *IEEE Trans. on IP*, 10(2): 266-277, 2001. *Pattern Recognition* 36(9): 1929-1943. 2003.
8. D. Cremers, F. Tischhauser, J. Weickert and C. Schnorr, "Diffusion Snakes: Introducing Statistical Shape Knowledge into the Mumford-Shah Functional", International Journal of Computer Vision 50(3): 295-313; Dec 2002
9. A. Dervieux and F. Thomasset "A finite element method for the simulation of Rayleigh-Taylor instability" *Lecture Notes in Mathematics*, 771:145–159, 1979
10. A. Dervieux and F. Thomasset "Multifluid incompressible flows by a finite element method" In *International Conference on Numerical Methods in Fluid Dynamics*, 158–163, 1980
11. C. Feddern, J. Weickert, B. Burgeth and M. Welk "Curvature-driven PDE methods for matrix-valued images.", Technical Report No. 104, Department of Mathematics, Saarland University, Saarbrücken, Germany, Apr. 2004.
12. W. Foerstner and E. Gulch, "A fast operator for detection and precise location of distinct points, corners and centres of circular features", in: Intercomm. Conf. on Fast Proc. of Photogrammetric. Data, Interlaken, June 1987, pp. 281-305.
13. C. Lenglet, M. Rousson, R. Deriche, and O. Faugeras, "Statistics on multivariate normal distributions: A geometric approach and its application to diffusion tensor mri," INRIA, Research Report 5242, Jun 2004.
14. C. Lenglet, M. Rousson, R. Deriche, and O. Faugeras, "Toward segmentation of 3D probability density fields by surface evolution: Application to diffusion mri," INRIA, Research Rep. 5243, June 2004.
15. C. Lenglet, M. Rousson, and R. Deriche, "Segmentation of 3d probability density fields by surface evolution: Application to diffusion mri," in *Proc. of the MICCAI*, Saint Malo, France, Sep. 2004.
16. M. E. Leventon, O. Faugeras, W. E. L. Grimson, and W. M. W. III, "Level set based segmentation with intensity and curvature priors," in *Proc. of the IEEE Workshop on MMBIA*, Hilton Head, SC, USAs, jun 2000, pp. 4–11.
17. R. de Luis-Garcia, R. Deriche, C. Lenglet, and M. Rousson, "Tensor processing for texture and colour segmentation," INRIA, Research. Rep., in press.
18. R. Malladi, J. A. Sethian, and B. C. Vemuri, "Shape modeling with front propagation: A level set approach," *IEEE Trans. on PAMI*, 17(2): 158-175, feb 1995.
19. N. Paragios and R. Deriche, "Geodesic active regions and level set methods for supervised texture segmentation," *The International Journal of Computer Vision*, 46(3): 223-247, 2002.
20. N. Paragios and R. Deriche, "Geodesic active regions: A new framework to deal with frame partition problems in computer vision," *Journal of Visual Communication and Image Representation*, vol. 13, pp. 249–268, 2002.
21. M. Rousson, T. Brox, and R. Deriche, "Active unsupervised texture segmentation on a diffusion based feature space," in *Proc. of CVPR*, Madison, Wisconsin, USA, jun 2003.

22. M. Rousson, C. Lenglet, and R. Deriche, "Level set and region based surface propagation for diffusion tensor mri segmentation," in *Proc. of the Computer Vision Approaches to Medical Image Analysis Workshop*, Prague, May 2004.
23. S. Osher and J. A. Sethian, "Fronts propagating with curvature dependent speed: Algorithms based on hamilton-jacobi formulation," *Journal of Computational Physics*, vol. 79, pp. 12–49, 1988.
24. Z. Wang and B. C. Vemuri, "An affine invariant tensor dissimilarity measure and its applications to tensor-valued image segmentation," in *Proc. of the IEEE CVPR*, Washington DC, USA, 2004, pp. 228–233.
25. Z. Wang and B. C.Vemuri, "Tensor field segmentation using region based active contour model," in *Proc. of the ECCV*, Prague, Czech Republic, may 2004.